Searching for new spin-dependent interactions with $SmCo_5$ spin sources and a spin-exchange-relaxation-free comagnetometer

W. Ji,[1] C. B. Fu,[2,*] and H. Gao[1,3,4,†]

[1]*Dept. of Phys., Tsinghua University, Beijing, 100084, China*
[2]*Institute of Nuclear and Particle Physics, Phys. & Astro. Dept., Shanghai Jiao Tong University, Shanghai, 200240, China*
[3]*Dept. of Phys., Duke University and Triangle Universities Nuclear Laboratory, Durham, North Carolina 27708, U.S.A*
[4]*Duke Kunshan University, Kunshan, Jiangsu, 215316, China*

(Received 30 October 2016; published 13 April 2017)

We propose a novel method to search for possible new macroscale spin- and/or velocity-dependent forces (SVDFs) based on specially designed $SmCo_5$ spin sources and a spin exchange relaxation-free (SERF) comagnetometer. A simulation shows that, by covering a $SmCo_5$ permanent magnet with a layer of pure iron, a high net spin density source of about $1 \times 10^{22}/\mathrm{cm}^3$ could be obtained. Taking advantages of the high spin density of this iron-shielded $SmCo_5$ and the high sensitivity of the SERF, the proposed method could set up new limits of greater than 10 orders of magnitude more sensitive than those from previous experiments or proposals in exploring SVDFs in force ranges larger than 1 cm.

DOI: 10.1103/PhysRevD.95.075014

I. INTRODUCTION

Searches for anomalous spin- and/or velocity-dependent forces (SVDFs) have drawn considerable attention in the past few decades. Various theories beyond the standard model have predicted weakly coupled scalar, pseudoscalar, vector, or axial-vector bosons with light masses[1–3]. It is believed that these light bosons may be the answers to many fundamental questions related to, for examples, the CP or CPT violation [4,5], Lorentz violation [6], and the dark matter [7] etc. Obviously, how to experimentally set limits on coupling constants of such bosons or even find them is an important step for human beings to further understand the mother Nature.

The light bosons, if they exist, can mediate long-range SVDFs between macroscopic objects [1]. Many highly sensitive experimental techniques have been employed to search for these new SVDFs, for examples, the torsion balance [8,9], the resonance spring [10,11], the spin exchange relaxation free (SERF) comagnetometer [12], and other nuclear magnetic resonance (NMR) based methods [13], etc.

In all these experimental techniques, the spin density of the source is one of the most critical factors. The force strength mediated by a boson having nonzero mass drops exponentially, for example [14],

$$V_2 = \frac{f_2 \hbar c}{4\pi}(\hat{\boldsymbol{\sigma}}_1 \cdot \hat{\boldsymbol{\sigma}}_2)\left(\frac{1}{r}\right)e^{-r/\lambda}, \tag{1}$$

where $\hat{\boldsymbol{\sigma}}_1, \hat{\boldsymbol{\sigma}}_2$ are the spins of the two particles respectively, λ is the interaction range, and r is the distance between the two particles. An effective magnetic field $B_{\mathrm{eff}} = f_2 \hbar c \hat{\boldsymbol{\sigma}}_2 e^{-r/\lambda}/(4\pi r)$ can be employed to detect the boson, and increasing the spin density of the source in the interaction range λ can significantly improve the detection sensitivity. Therefore, various methods have been employed to improve the spin densities [15–17].

In this paper we propose a new specially designed high spin density material, an iron-shielded $SmCo_5$ permanent magnet (ISSC) together with a SERF comagnetometer to constrain the coupling strengths of the various terms in SVDFs [14]. In the following sections of this paper, we will give an overview of the proposed setup first, and then a short introduction of the SERF comagnetometer. The structure of the ISSC and its finite element analysis (FEA) simulation are provided. Then the comparisons between the sensitivities of this proposal and others will be presented. The limits on the coupling strengths set by this proposal could be improved by as large as more than 10 orders of magnitude compared with those from the previous experiments or proposals.

II. EXPERIMENTAL SETUP

The proposed setup is shown in Fig. 1 schematically. The left side is a SERF comagnetometer [18]. ^{3}He and K sealed in a glass cell will be polarized and serve as the force probes for the exotic two-body interactions. As part of the SERF comagnetometer, several layers of μ-metal cover the K-^{3}He glass cell to reduce the possible ambient magnetic fields, and make the system work in the so-called SERF regime. The right side in Fig. 1 is the iron-shielded $SmCo_5$ (ISSC). The ISSC can move in different ways, which will be introduced in details later. The ISSCs are also covered with

*Corresponding author: cbfu@sjtu.edu.cn
†Corresponding author: gao@phys.duke.edu

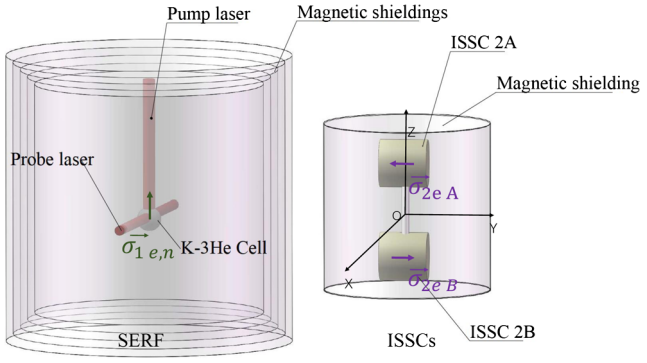

FIG. 1. The schematic view of the proposed experiment. The neutrons in polarized ^{3}He serve as $\vec{\sigma}_{1n}$; the electrons in polarized K serve as $\vec{\sigma}_{1e}$. Two ISSC spin sources, 2A and 2B, serve as $\vec{\sigma}^A_{2e}$ and $\vec{\sigma}^B_{2e}$. By rotating the ISSCs with a given frequency f_0 and then locking onto that frequency in the SERF spectra, the noises can be reduced, and then the detecting sensitivities can be highly improved. Depending on different terms of the SVDF under testing, the directions of $\vec{\sigma}^A_{2e}$ and $\vec{\sigma}^B_{2e}$ could be put along x, y, or z-direction, and the ISSCs can rotate along x or y axis (see text and Table I for details).

μ-metals to further reduce the magnetic flux leakage from the $SmCo_5$ even after the iron-shielding.

A. SERF comagnetometer

To get a SERF comagnetometer work, the glass cell is normally heated to about 160°C to achieve a sufficiently high alkali vapor density. The leading order of the alkali atoms' polarization in x direction is given by [12]:

$$P^e_x = \frac{P^e_z \gamma_e}{R_{\rm tot}}(b^n_y - b^e_y), \tag{2}$$

where P^e_i is K electrons' polarization along the i-axis, b^n_y and b^e_y are the magneticlike field in y direction seen by the ^{3}He nucleus and the K electrons, respectively, $R_{\rm tot}$ is the K electron's relaxation rate, and γ_e is the gyromagnetic ratio for the K electrons. Therefore, if the SVDFs exist, and couple to neutrons or electrons, the corresponding effective fields b^n_y or b^e_y can be detected by the SERF comagnetometer. SERF comagnetometers represent the most sensitive magnetometer today [12,19].

B. Iron-shielded $SmCo_5$

A higher spin density means a higher sensitivity in the SVDF searching. Permanent magnets have high spin densities. However, a permanent magnet's field can cause large background signals in a SVDF-search experiment if used directly. To overcome this, we designed a new structure shown in Fig. 2. At its center, there is a cylindrical $SmCo_5$ magnet. Then the $SmCo_5$ cylinder is covered by a layer of pure iron to shield the magnetic field from the $SmCo_5$ core.

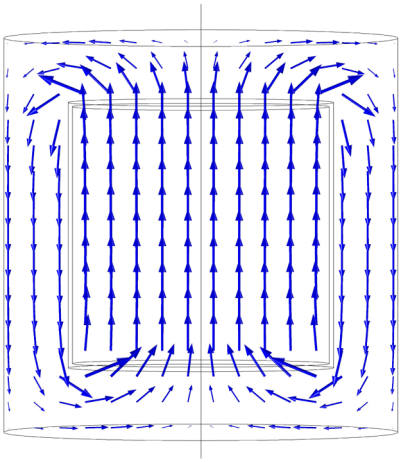

FIG. 2. A schematic diagram of a spin source and its FEA simulation results. From inside to outside, there are layers of $SmCo_5$ magnet, air gap, and pure iron. The blue arrows represents the magnetic field. In the simulation, the sizes of $SmCo_5$ are set to be $\pi \times 15^2 \times 30$ cm^3, and outside pure irons are set to be 7.5 cm thick.

The total electron spin density of ISSC is contributed by two parts: $SmCo_5$ ($\boldsymbol{n}_{SmCo_5}$) and iron shielding ($\boldsymbol{n}_{\rm iron}$). The magnetic moment of the Sm^{3+} ion is very small at room temperature compared with five cobalt ions, i.e. $-0.04\mu_B$ vs. $-8.97\mu_B$ [20,21]. It is safe to ignore the magnetization of Sm in the $SmCo_5$. Therefore the electron spin density of $SmCo_5$ can be written as [20],

$$\boldsymbol{n}_{\rm SmCo} = \frac{f_{\rm Co}(1+R)}{\mu_B}\mathbf{M}_{\rm Co}, \tag{3}$$

where $\mathbf{M}_{\rm Co}$ is the magnetization of Co, $f_{\rm Co} = 0.80 \pm 0.004$ [20] is the spin contribution of the magnetic moments of Co, $R = -0.36$ [20] is the spin ratio of Sm to Co, and μ_B is the Bohr magneton. The minus sign of R means that the Sm spins are in the opposite direction of Co. For $SmCo_5$ magnetized to 10 kGs, its spin density is about $\boldsymbol{n}_{\rm SmCo} = 4.5 \times 10^{22}/{\rm cm}^3$.

The electron spin density of the pure iron can be calculated in the similar way as Eq. (3).

$$\boldsymbol{n}_{\rm Fe} = \frac{f_{\rm Fe}}{\mu_B}\mathbf{M}_{\rm Fe}, \tag{4}$$

where $\mathbf{M}_{\rm Fe}$ is the magnetization of the iron, $f_{\rm Fe} = 0.957$ is the spin contribution of the magnetic moments in Fe [22,23]. The magnetism in pure iron mainly comes from the spin magnetic moment of the $3d$ electrons because the orbital magnetic moment of the $3d$ electrons can be quenched in the inhomogeneous crystalline electric field [24]. For pure iron magnetized to 10 kGs, its spin density is about $\boldsymbol{n}_{\rm Fe} = 8.2 \times 10^{22}/{\rm cm}^3$.

Even μ-metals may have higher spin densities [25], we prefer pure iron due to its simple structure which potentially affects the data analysis of the SVDF searching experiments.

C. FEA Simulation

With the FEA method, we simulated the magnetization distribution and then the spin density distributions in the ISSC. The main optimized input parameters are listed in Table II. The structure under simulation is shown in Fig. 2. The "net" electron spin of this ISSC can be written as $\boldsymbol{N}_{\rm net} = \int \boldsymbol{n}_{\rm SmCo} {\rm d}V_{\rm SmCo} + \int \boldsymbol{n}_{\rm Fe} {\rm d}V_{\rm Fe}$, where $V_{\rm SmCo}$ and $V_{\rm Fe}$ are the volumes of $SmCo_5$ and Iron, respectively. According to the FEA simulation (shown in Table II), the net electron spin of this structure is $8 \times 10^{26}\hbar/2$, while at the same time the magnetic field can be canceled to very close to zero (<0.5 Gs at a distance 5 cm away from the pure iron).

This special feature is mainly due to the fact that Sm's $4f$ electrons and Co's $3d$ electrons in $SmCo_5$ have large orbital magnetic moments, while Fe $3d$ electrons' orbital magnetic moments are quenched. Therefore, it is possible to reduce the outside magnetic field close to zero, while at the same time keep the total net electron spins nonzero.

There are some other spin materials which are chosen or proposed for SVDF searches, for example, Alnico, dysprosium iron garnet (DyIG), and GGG etc. [17,26,27]. The Alnico has higher spin densities, but its orbital magnetic moment is too low [20] to benefit this experiment. The garnet-DyIG and GGG crystals have also been used in the SVDF search experiments. However, fabrication of those crystals are difficult, especially for large-size crystals, which limits their applications. Due to the simple structure, stable property, and high spin density, the ISSC is an excellent spin material for SVDF searches.

D. Error analysis

To achieve the best sensitivity, the rotation frequency of the ISSC can be optimized by carefully taking into account both the laboratory background noise level and the rotating velocity. For a SERF magnetometer in a specific laboratory, its sensitivity is different at different frequency. On the other hand, for the velocity-dependent forces, normally the higher the velocity, which means the higher frequency in the proposed setup, the higher the sensitivity is. Therefore, the rotation frequency can be optimized accordingly. A SERF sensitivity of $\rm fT/Hz^{1/2}$ level can be achieved routinely in a typical laboratory environment at a frequency of several Hz [19]. A detailed error analysis of the SERF magnetometer itself can be found in Ref. [12].

Because the ISSCs are rotating periodically, one can remove the background noise by taking the difference between the maximum and minimum values of the SVDF signals under investigation in one rotation period. Furthermore, for a time interval larger than one period, the non-linear long-term background fluctuations can also be removed in a similar way, as is shown in Ref. [28]. The background fluctuations here include temperature fluctuations of the SERF, and the ambient magnetic field fluctuation in the lab, etc.

The normal magnetic field leakage of the ISSCs is the most important systematic error because it has the same frequency as that of the SVDFs signals, and cannot be filtered out after applying the ISSCs' rotating frequency. As the FEA simulation shows above, the leakage of ISSCs is less than 5×10^{-5} T. The static magnetic shielding of the ISSCs provides a suppression factor better than 10^6, and the SERF's magnetic shielding provides an additional suppression factor of greater than 10^6. The distance of 20 cm from the ISSCs to the SERF's cell will reduce the ISSC's magnetic field by at least a factor 10^3. Therefore, the magnetic field leakage of ISSCs into the SERF signals is estimated to be smaller then 1 aT. Furthermore, if a higher sensitivity is needed, it is easy to add more static μ-metal shielding between the ISSC and the SERF's magnetic shielding.

III. ESTIMATIONS OF NEW LIMITS FOR SVDFS

By using the ISSC designed above and a SERF comagnetometer, the sensitivities of SVDF searches could be estimated.

Mathematically, there are 16 terms of SVDFs [14], Here we list the representative 8 terms which are spin-dependent [V_2 in Eq. (1), V_3, V_{9+10}, and V_{11}] as well as spin-and-velocity-dependent forces (V_{6+7}, V_{14}, V_{15}, and V_{16}):

$$V_3 = \frac{f_3\hbar^3}{4\pi m_1 m_2 c}\left[(\hat{\boldsymbol{\sigma}}_1\cdot\hat{\boldsymbol{\sigma}}_2)\left(\frac{1}{\lambda r^2}+\frac{1}{r^3}\right) - (\hat{\boldsymbol{\sigma}}_1\cdot\hat{\boldsymbol{r}})(\hat{\boldsymbol{\sigma}}_2\cdot\hat{\boldsymbol{r}})\left(\frac{1}{\lambda^2 r}+\frac{3}{\lambda r^2}+\frac{3}{r^3}\right)\right]e^{-r/\lambda}, \quad (5)$$

$$V_{6+7} = -\frac{f_{6+7}\hbar^2}{4\pi m_\mu c}[(\hat{\boldsymbol{\sigma}}_1\cdot\mathbf{v})(\hat{\boldsymbol{\sigma}}_2\cdot\hat{\boldsymbol{r}})]\left(\frac{1}{\lambda r}+\frac{1}{r^2}\right)e^{-r/\lambda}, \quad (6)$$

$$V_{9+10} = \frac{f_{9+10}\hbar^2}{8\pi m_\mu}(\hat{\boldsymbol{\sigma}}_1\cdot\hat{\boldsymbol{r}})\left(\frac{1}{r\lambda}+\frac{1}{r^2}\right)e^{-r/\lambda}, \quad (7)$$

$$V_{11} = -\frac{f_{11}\hbar^2}{4\pi m_\mu}[(\hat{\boldsymbol{\sigma}}_1\times\hat{\boldsymbol{\sigma}}_2)\cdot\hat{\boldsymbol{r}}]\left(\frac{1}{r\lambda}+\frac{1}{r^2}\right)e^{-r/\lambda}, \quad (8)$$

$$V_{14} = \frac{f_{14}\hbar}{4\pi}[(\hat{\boldsymbol{\sigma}}_1\times\hat{\boldsymbol{\sigma}}_2)\cdot\mathbf{v}]\left(\frac{1}{r}\right)e^{-r/\lambda}, \quad (9)$$

$$V_{15} = -\frac{f_{15}\hbar^3}{8\pi m_1 m_2 c^2}\{(\hat{\boldsymbol{\sigma}}_2\cdot\hat{\boldsymbol{r}})[\hat{\boldsymbol{\sigma}}_1\cdot(\mathbf{v}\times\hat{\boldsymbol{r}})] + (\hat{\boldsymbol{\sigma}}_1\cdot\hat{\boldsymbol{r}}) \times[\hat{\boldsymbol{\sigma}}_2\cdot(\mathbf{v}\times\hat{\boldsymbol{r}})]\}\left(\frac{1}{\lambda^2 r}+\frac{3}{\lambda r^2}+\frac{3}{r^3}\right)e^{-r/\lambda}, \quad (10)$$

$$V_{16} = -\frac{f_{16}\hbar^2}{8\pi m_\mu c^2}\{(\hat{\boldsymbol{\sigma}}_2\cdot\mathbf{v})[\hat{\boldsymbol{\sigma}}_1\cdot(\mathbf{v}\times\hat{\boldsymbol{r}})] + (\hat{\boldsymbol{\sigma}}_1\cdot\mathbf{v})[\hat{\boldsymbol{\sigma}}_2\cdot(\mathbf{v}\times\hat{\boldsymbol{r}})]\}\left(\frac{1}{\lambda r}+\frac{1}{r^2}\right)e^{-r/\lambda}, \quad (11)$$

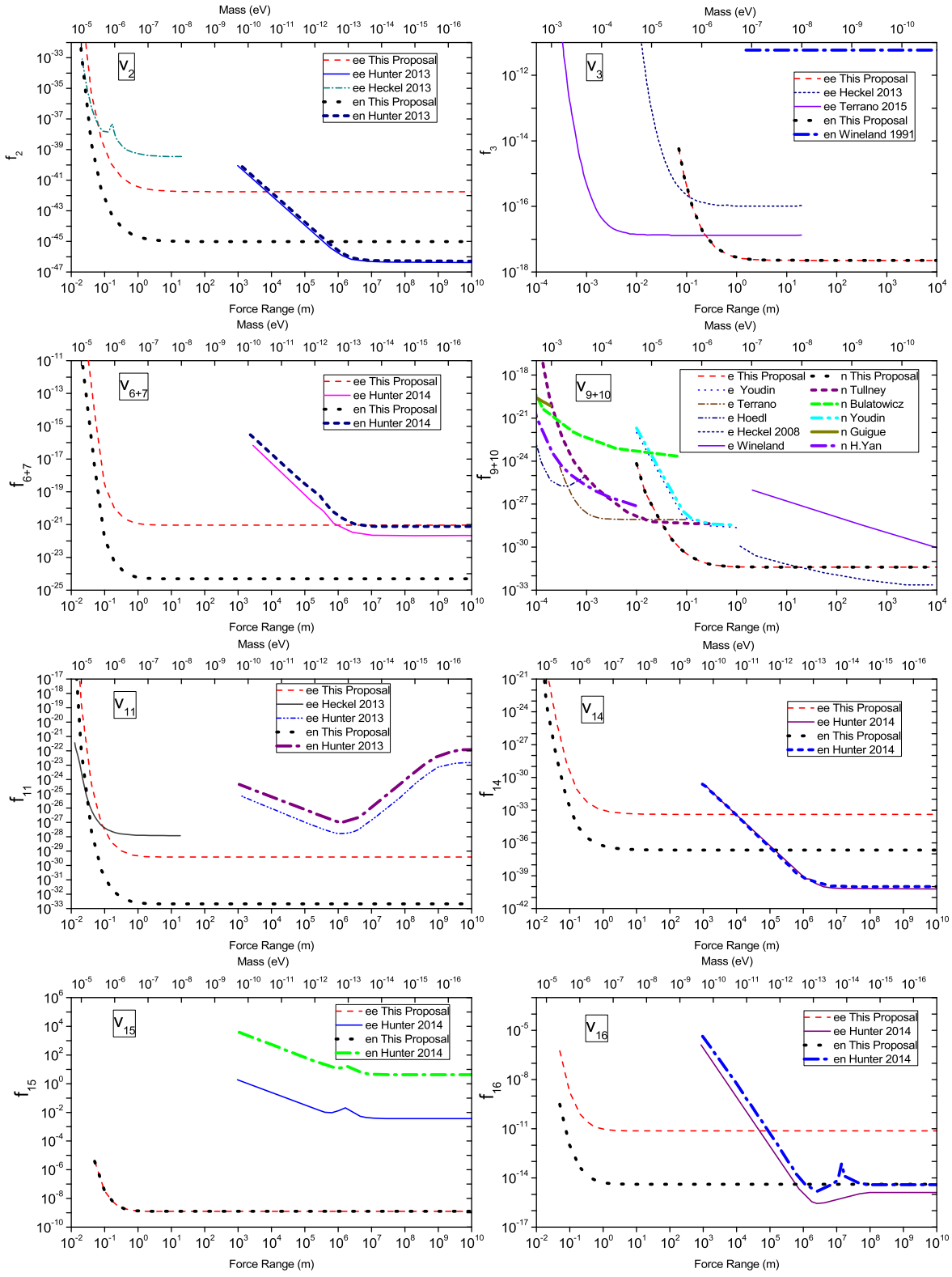

FIG. 3. Comparisons of the limits set by this proposal and others in literatures. The input parameters, which are conservatively assumed, are shown in Tables I and II. The "*ee*" ("*en*") labeled here means the coupling between electron and electron (neutron). The label "*e*" ("*n*") in figure for f_{9+10} means coupling between unpolarized mass and electron (neutron). The references for different terms of the SVDFs are: V_2 from Ref. [32–34], V_3 from Refs. [26,31,32,34], V_{6+7}, V_{14}, V_{15} and V_{16} from Ref. [30], V_{9+10} are from Refs. [20,26,35–44], and V_{11} from Ref. [32,33].

TABLE I. The optimized rotating axises and orientations of $\vec{\sigma}_{2e}^{A}$ and $\vec{\sigma}_{2e}^{B}$ when estimate the sensitivities of the different SVDF terms with the proposed setup.

Terms	V_2	V_3	V_{9+10}	V_{11}	V_{6+7}	V_{14}	V_{15}	V_{16}
Rotating axis	y	y	x	y	x	y	y	y
$\vec{\sigma}_{2e}^{A}$	$+z$	$+x$	$+z$	$+z$	$+y$	$+y$	$+z$	$+x$
$\vec{\sigma}_{2e}^{B}$	$+z$	$+x$	$+z$	$+z$	$-y$	$-y$	$+z$	$-x$

TABLE II. Input parameters for the FEA simulation.

Parameter	value
The SERF's center to the ISSCs' center	0.7 m
Distance between the two ISSCs	0.6 m
Rotating frequency	5 Hz
Soft iron's relative permeability	12000
$SmCo_5$ magnetization	10 kGs
The SERF's sensitivity	1 fT/Hz$^{1/2}$
Data taking time	2 weeks
The soft Iron's nucleon density	4.7×10^{24} cm^{-3}
The $SmCo_5$'s nucleon density	5.1×10^{24} cm^{-3}

where f_i is the dimensionless coupling constant between particles, m_1 and m_2 are their respective masses, m_μ is their reduced mass.

By optimizing the rotational axes of the ISSCs, one can obtain maximum sensitivities for different terms of the SVDFs. The ISSCs rotational axes for different SVDF terms are listed in Table I. The main input parameters, which are conservative, are listed in Table II.

According to Eq. (2), we take the effective magnetic field for electron as $B_{\rm eff}^{(e)} = b_y^e$, while for neutron, $B_{\rm eff}^{(n)} = b_y^n/0.87$, due to the limited neutron polarization of 87% in a ^{3}He nucleus [12,29].

The estimated results are shown in Fig. 3. In $\lambda > 0.1$ m, even with conservative input parameters, the proposed method could highly improve the sensitivities of these types of the SVDF searches. For example, the limits of $f_{15}^{(en)}$, and $f_{16}^{(en)}$ can be improved by over 10 orders of magnitude in $\lambda < 1000$ m compared with the current best limits [30]. For the constraints of the possible new "dipole-dipole interaction" $f_3^{(en)}$ and $f_{6+7}^{(en)}$, this proposal could be more than 7 orders of magnitude better than the current records [30,31] at around $\lambda = 1000$ m. For the limits of f_{9+10} and $f_2^{(en)}$, this proposal could be more than over 3 orders of magnitude better than other proposals [17,27]. For other terms of the SVDFs for electron-electron (ee) and electron-nucleon (en) couplings, the proposed method can also be several orders of magnitude better than other corresponding best limits up to date.

IV. SUMMARY

The experimental searches for new macro scale SVDFs are important for testing theories beyond the standard model. High spin density and easily handling materials are critical for SVDF-search experiments. We propose the ISSC structure, i.e. a $SmCo_5$ permanent magnet covered with pure iron, for the SVDF studies. In this new structure, the magnetic field could be highly reduced, while at the same time a large amount of net electron spin polarization can be achieved. By using this ISSC structure, together with the highly sensitive SERF comagnetometer, the sensitivities for detecting different terms of SVDFs are discussed. This new approach has sensitivities as large as 10 orders of magnitude higher compared with those from previous experiments or proposals, which makes it a promising method in new experiments searching for spin-dependent interactions.

ACKNOWLEDGMENTS

This work is supported by the National Nature Science Foundation of China (Grant No. 11375114), and the U.S. Department of Energy under Contract No. DE-FG02-03ER41231. We thank Y. Chen for useful discussion on SERF magnetometers. One of us (C. B. F.) thanks Shanghai Municipal Science and Technology Commission for the supports (under Grant No. 11DZ2260700).

[1] J. Jaeckel and A. Ringwald, Annu. Rev. Nucl. Part. Sci. **60**, 405 (2010).
[2] R. D. Peccei and H. R. Quinn, Phys. Rev. Lett. **38**, 1440 (1977).
[3] C. T. Hill and G. G. Ross, Nucl. Phys. **B311**, 253 (1988).
[4] J. Leitner and S. Okubo, Phys. Rev. **136**, B1542 (1964).
[5] J. E. Kim and G. Carosi, Rev. Mod. Phys. **82**, 557 (2010).
[6] C.-G. Shao, Y.-J. Tan, W.-H. Tan *et al.*, Phys. Rev. Lett. **117**, 071102 (2016).
[7] L. Covi, H. Kim, J. Kim, and L. Roszkowski, J High Eng. Phys. 05 (**2001**) 033.
[8] R. C. Ritter, C. E. Goldblum, W. T. Ni, G. T. Gillies, and C. C. Speake, Phys. Rev. D **42**, 977 (1990).
[9] B. R. Heckel, C. E. Cramer, T. S. Cook *et al.*, Phys. Rev. Lett. **97**, 021603 (2006).

[10] J. Long, H. Chan, A. Churnside *et al.*, Nature (London) **421**, 922 (2003).
[11] J. C. Long and V. A. Kostelecký, Phys. Rev. D **91**, 092003 (2015).
[12] G. Vasilakis, J. M. Brown, T. W. Kornack, and M. V. Romalis, Phys. Rev. Lett. **103**, 261801 (2009).
[13] H. Yan, G. Sun, S. Peng *et al.*, Phys. Rev. Lett. **115**, 182001 (2015).
[14] B. A. Dobrescu and I. Mocioiu, J High Energy Phys. 11 (**2006**) 005.
[15] T. G. Walker and W. Happer, Rev. Mod. Phys. **69**, 629 (1997).
[16] S. Afach, G. Ban, G. Bison *et al.*, Phys. Lett. B **745**, 58 (2015).
[17] P.-H. Chu, E. Weisman, C.-Y. Liu, and J. C. Long, Phys. Rev. D **91**, 102006 (2015).
[18] J. C. Allred, R. N. Lyman, T. W. Kornack, and M. V. Romalis, Phys. Rev. Lett. **89**, 130801 (2002).
[19] H. Dang, A. Maloof, and M. Romalis, Appl. Phys. Lett. **97**, 151110 (2010).
[20] B. R. Heckel, E. G. Adelberger, C. E. Cramer *et al.*, Phys. Rev. D **78**, 092006 (2008).
[21] D. Givord, J. Laforest, J. Schweizer, and F. Tasset, J. Appl. Phys. **50**, 2008 (1979).
[22] M. Seavey Jr and P. Tannenwald, J. Appl. Phys. **29**, 292 (1958).
[23] Z. Frait and R. Gemperle, Le Journal de Physique Colloques **32**, C1 (1971).
[24] R. M. Bozorth, *Ferromagnetism* (Wiley-VCH, New York, 1993), Vol. 1, p. 992, ISBN 0-7803-1032-2.
[25] J. M. Shaw, H. T. Nembach, T. Silva, and C. T. Boone, J. Appl. Phys. **114**, 243906 (2013).
[26] W. A. Terrano, E. G. Adelberger, J. G. Lee, and B. R. Heckel, Phys. Rev. Lett. **115**, 201801 (2015).
[27] T. M. Leslie, E. Weisman, R. Khatiwada, and J. C. Long, Phys. Rev. D **89**, 114022 (2014).
[28] H. E. Swanson and S. Schlamminger, Meas. Sci. Technol. **21**, 115104 (2010).
[29] J. L. Friar, B. F. Gibson, G. L. Payne, A. M. Bernstein, and T. E. Chupp, Phys. Rev. C **42**, 2310 (1990).
[30] L. R. Hunter and D. G. Ang, Phys. Rev. Lett. **112**, 091803 (2014).
[31] D. J. Wineland, J. J. Bollinger, D. J. Heinzen, W. M. Itano, and M. G. Raizen, Phys. Rev. Lett. **67**, 1735 (1991).
[32] B. R. Heckel, W. A. Terrano, and E. G. Adelberger, Phys. Rev. Lett. **111**, 151802 (2013).
[33] L. Hunter, J. Gordon, S. Peck *et al.*, Science **339**, 928 (2013).
[34] S. Kotler, R. Ozeri, and D. F. J. Kimball, Phys. Rev. Lett. **115**, 081801 (2015).
[35] A. N. Youdin, D. Krause Jr, K. Jagannathan, L. R. Hunter, and S. K. Lamoreaux, Phys. Rev. Lett. **77**, 2170 (1996).
[36] W.-T. Ni, S.-S. Pan, H.-C. Yeh, L.-S. Hou, and J. Wan, Phys. Rev. Lett. **82**, 2439 (1999).
[37] G. D. Hammond, C. C. Speake, C. Trenkel, and A. P. Patón, Phys. Rev. Lett. **98**, 081101 (2007).
[38] S. A. Hoedl, F. Fleischer, E. G. Adelberger, and B. R. Heckel, Phys. Rev. Lett. **106**, 041801 (2011).
[39] K. Tullney, F. Allmendinger, M. Burghoff *et al.*, Phys. Rev. Lett. **111**, 100801 (2013).
[40] A. P. Serebrov, O. Zimmer, P. Geltenbort, A. Fomin *et al.*, JETP Lett. **91**, 6 (2010).
[41] A. K. Petukhov, G. Pignol, D. Jullien, and K. H. Andersen, Phys. Rev. Lett. **105**, 170401 (2010).
[42] M. Bulatowicz, R. Griffith, M. Larsen *et al.*, Phys. Rev. Lett. **111**, 102001 (2013).
[43] P.-H. Chu, A. Dennis, C. Fu *et al.*, Phys. Rev. D **87**, 011105 (2013).
[44] H. Yan *et al.*, Eur. Phys. J. C **74**, 1 (2014).